Materials Research. 2017; 20(2): 523-531
DOI: http://dx.doi.org/10.1590/1980-5373-MR-2016-0662

Electronic Effect of V, Ti, and Sc Impurities on the Hyperfine Interactions of Fe Atoms in α-Fe: A First Principles Study

***Carlos Ariel Samudio Pérez*[a]*, Antônio Vanderlei dos Santos*[b]**

[a] *Instituto de Ciências Exatas, Universidade de Passo Fundo, Campus de Passo Fundo, 99001-970, Passo Fundo, RS, Brazil*
[b] *Universidade Regional Integrada do Alto Uruguai e das Missões, Campus Santo Ângelo, 98802-470, Santo Ângelo, RS, Brazil*

Received: September 13, 2016; Revised: December 18, 2016; Accepted: February 02, 2017

The Linearized Augmented Plane Wave method, as implemented in the Wien2k computational code, was used to investigate the effects of the 3d transition metals (TM) Sc, Ti, and V impurities on the hyperfine interaction of iron atoms in α-Fe. The calculation results of this study suggest that the introduction of a TM (TM = Sc, Ti, and V) impurity into α-Fe increases the size of the lattice as well as alters the electronic charge distribution between the atoms in the lattice and at the atomic sphere of the host Fe atoms. The increase of the lattice disturbs the position of the iron atoms and the change on the electronic distribution disturbs the hyperfine interactions at all iron nuclei. The disturbances on the hyperfine magnetic field, isomer shift and electric field gradient at the iron nuclei depend on its relative location to the impurity atom.

Keywords: *electronic structure, ferromagnetic, magnetic properties*

1. Introduction

Iron and iron-based alloys are of great importance for a variety of technological applications. Nowadays, iron alloys with transition metals (TM) play a fundamental role for designing and manufacturing specialty steels, some of them are strong candidates to structural materials for both fission and fusion applications due to their good tolerance to strong neutron irradiation[1]. At room temperature and atmospheric pressure, pure iron is found in the form of α-Fe with a body-centered cubic (bcc) structure and magnetic ground state of ferromagnetic character[2]. The magnetic anisotropy of α-Fe is very low, with easy magnetization axes parallel to (100) direction and the magnetic moment for iron atoms is well localized. The internal hyperfine field on the iron nucleus originates mainly due to the Fermi contact interaction, once for cubic symmetry and neglecting spin–orbit interaction the dipolar and orbital contribution vanishes[3]. The electric field gradient vanishes on the iron nuclei due to the cubic symmetry.

The fundamental properties of iron can be drastically modified by the addition of impurities. The nature and magnitude of the changes in the iron properties are sensitive to the electronic character of the alloying element, to their concentration, and to the alloy manufacturing process. In fact, the substitution of Fe atoms by an impurity into Fe matrix can produce local lattice disturbance and modify the mechanical, electrical, and magnetic properties of host Fe[4]. Especially, the local magnetic behavior of Fe atoms is quite sensitive to the structural and chemical environment of the atoms. The addition of impurity atoms to α-Fe causes a disturbance of the electron spin and charge density in the interstitial regions of the lattice and at the atom sites. In turn, this disturbance can lead to changes in the hyperfine interactions at the iron nuclei. The changes in the hyperfine magnetic field, the isomer shift and the electric quadrupole interaction at the iron sites can be studied by experimental techniques as Mossbauer spectroscopy of ^{57}Fe[5-7].

From the point of view of magnetism the heavier 3d TM on the right side of the series, Fe, Co, and Ni are ferromagnetic, Cr and Mn in the center of the series are antiferromagnetic, whereas the lightest elements on the left-hand of the 3d series Sc, Ti and V, have nonmagnetic ground state. The alloying of 3d TM between themselves often gives rise to very interesting fundamental physical properties. For example, Fe-Ni alloy system shows several interesting effects, as Invar (alloys with very low values of the linear expansion temperature coefficient), and Permalloy (soft magnetic materials with a very high magnetic permeability), which attracted attention because of technological applications. Such alloys have been the subject of many theoretical and experimental investigations[8-11].

Currently there are several manufacturing techniques for the preparation of alloy samples in bulk or nanosized structure, as well as in crystalline or amorphous form. This has promoted the design and research of new materials and related properties. Special interest has been devoted to the investigation of low-dimensional systems, as nanoparticles, surfaces, and multilayers, for the reason that their magnetic

* e-mail: samudio@upf.br

and electronic structures, differ from those of the bulk samples with equal chemical composition. The research on new materials has also stimulated theoretical and experimental studies of iron-based 3d TM alloys because of their variety of structural and magnetic properties and potential applications in high strength steels and suitability for high corrosion resistance. One of the first steps towards understanding the fundamental physical properties of these new materials is the prediction of the ground state properties via first principles studies. In this sense, ab-initio computational methods based on density functional theory (DFT) have proven to be useful tools for accurately modeling fundamental properties (i.e., formation and cohesive energies, magnetic moment and hyperfine interactions) of new materials[12].

The iron-based alloys TM play an important role in steel production because many of the main characteristics of these steels are tailored by controlling the concentration of the alloying elements in the bcc-Fe matrix. In order to understand how the 3d transition elements provide different properties to the Fe-based alloys, having knowledge about the effect of these elements on the fundamental properties of α-Fe is essential. Although, a large number of theoretical studies concerning to the electronic structure and magnetic properties of dilute alloys of TM in α-Fe have been reported[13-23], in a small number of these studies the atomistic simulation was based on the DFT. The DFT is one of the most important quantum-mechanical methods used in Chemistry and in Physic to calculate the electronic structure of atoms, molecules and solids[24]. On the other hand, in most of the studies conducted in these types of dilute alloys, mainly those in which the impurities are early 3d TM, the bulk magnetic behavior of the alloys has been interpreted as a simple dilution process in which the three Fe nearest neighbors to the TM are dominant. It has not been given much attention to the effect of the TM impurity on the changes of the electronic properties of the farthest irons. Hence, the objective of this study was to investigate via first principles calculations based on DFT the effects of 3d TM (TM = Sc, Ti, and V) impurities on the ground state properties of α-Fe. Special care has been devoted to the effect of the impurity on the change of the charge and spin density of iron atoms occupying all nonequivalent structural sites.

2. Computational method and structure

The calculations were performed with the linearized augmented plane wave (LAPW) method in the DFT framework. The electron exchange and correlation energy were calculated using the Perdew, Burke and Ernzerhof[25] parametrization within the Generalized Gradient Approximation (PBE-GGA)[26]. The method was used as implemented in the Wien2k computational code[27].

Theoretical calculations were performed for α-Fe(TM) (TM = Sc, Ti, and V) alloys modeled with a 3x3x3 supercell constructed with a unit cell of body-centered cubic (bcc) type and space group (Figure 1). The supercell contains 54 atoms, one TM impurity is located at the body-centered position (½,½,½) of the supercell and is surrounded by 53 Fe atoms. The composition of the supercell (TM_1Fe_{53}) corresponds to a concentration of 1.85 at. % of TM in α-Fe. The iron atoms are distributed in seven nonequivalent sites that will be identified as Fe1, Fe2, Fe3, Fe4, Fe5, Fe6, and Fe7, according to the iron localization at one of the seven sequential neighbor shells. The relative distance $r' = r/a$ (normalized by a, the lattice parameter of the bcc unit cell) from the impurity to particular neighbor shell is given on Table 1.

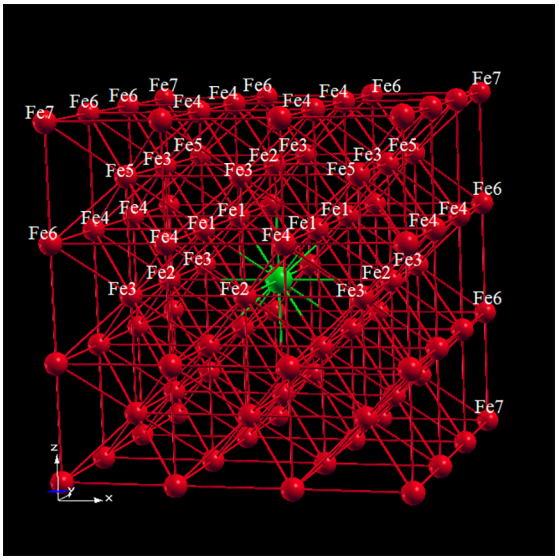

Figure 1. Lattice structure of the 3x3x3 supercell.

Table 1. Relative distance $r' = r/a$ (normalized by the lattice constant a) from TM impurity to non-equivalente iron sites in the 3x3x3 supercell structure. N stand for the number of all atoms in corresponding neighbors shell (distance r').

	$r' = r/a$	N
TM site	0	
Fe1	0.866	8
Fe2	1.000	6
Fe3	1.414	12
Fe4	1.658	24
Fe5	1.732	8
Fe6	2.179	24
Fe7	2.598	32

In the LAPW method, the electronic wave function was expanded in spherical harmonics inside the non-overlapping spheres centered at each nuclear position and in plane waves in the interstitial region of the unit cell. The convergence was controlled by a cut-off parameter $R_{mt}K_{max}$, where R_{mt} was the smallest atomic sphere radius and K_{max} the plane wave cut-off. In the present work the R_{mt} of particular atoms

were set to conform to the criterion of almost-touching spheres: 2.31 a.u for Fe, and 2.26 a.u. for TM = Sc, Ti, and V, respectively. The cut-off parameter ($R_{mt}K_{max}$) was fixed at -7 Ry. The wave functions within the atomic spheres are expanded in spherical harmonics with maximum multipolarity $l_{max} = 10$. The charge density was Fourier expanded up to $G_{max} = 12$. The Brillouin zone integrations were performed with the tetrahedron method in a grid (9 x 9 x 9) with 35 *k*-points. The theoretical calculations were performed in the non-magnetic (NM) and in ferromagnetic (FM) states and the self-consistency of the calculations was ascertained from the energy convergence criterion set to be 0.01 mRy.

3. Results and discussion

3.1 Ground state cohesive properties

The first principles calculations of the cohesive energy (E_c) as function of the cell volume, for the α-Fe(TM) (TM = Sc, Ti and V) alloys were performed by using the following equation:

$$E_c(\alpha - Fe(TM)) = E_T(\alpha - Fe(TM) - \Sigma_i n_i E_i \quad (1)$$

in this, E_T is the total energy of the supercell and, E_i correspond to the energy of each constituent *i* atom in its free state, both calculated from first principles. The determination of the magnetic ground state of each alloy was made by comparing the equilibrium (minimum) cohesive energy in the NM and FM states. From the cohesive energy point of view, all the alloys are more stable in the FM state (Table 2). In comparison, calculations were performed also for α-Fe (Table 2). The E_c value for α-Fe is in agreement with previous theoretical result: - 6.5 eV/at[28] and – 6.56 eV/at [29]. As it can be observed the E_c values for α-Fe(TM) (TM = Sc, Ti and V) alloys are higher than α-Fe, consequently the stability of the iron increases by the introduction of a TM impurity.

Table 2. The ground state cohesive energy (E_c), formation energy (E_f), bulk modulus (B) and lattice constant (a) for α-Fe(TM) (TM = Sc, Ti and V

α-Fe (TM)	*a* (Å)	*B* (GPa)	E_c (eV/atm) FM	E_c (eV/atm) NM	E_f (eV/atm) FM
α-Fe(Sc)	2.844	186.971	-6.318	-5.823	-0.047
α-Fe(Ti)	2.839	187.740	-6.360	-5.884	-0.080
α-Fe(V)	2.837	187.166	-6.400	-5.911	-0.081
α-Fe	2.835	197.242	-6.280		

The formation energy (E_f) in the FM state was calculated as a function of pure elements (Fe, TM = Sc, Ti, and V) through the equation

$$E_f(\alpha - Fe(TM)) = (E_T(\alpha - Fe(TM) - [53\, E_T(Fe) - E_T(TM)])/54 \quad (2)$$

where $E_T(i)$ is the total energy of the *i* atom (*i* = Fe, and TM) in bulk and at the ground state (0 K and 0 Pa), also calculated by first principles. Here it is assumed that E_f is equal to the formation enthalpy. The negative sign of E_f (Table 2) indicate the need to provide energy to form the alloy. The alloy that requires the smallest amount of energy for its formation is α-Fe(Sc).

The (E_c vs. cell volume) curve was used to determine the ground state structural properties: lattice parameter *a* (relative to the bcc unit cell) and bulk modulus B, for each α-Fe(TM) (TM = Sc, Ti and V) alloy, Table 2. The *a* value for α-Fe is in agreement with previous theoretical results reported by Rahman et. al.[11] and Błachowski et. al.[22], 2.83 Å, but is about 1 % lower than the experimental value, 2.867 Å[23]. As can be observed, the inclusion of the 3d TM impurity in α-Fe, leads to an increase of the lattice constant. The calculated bulk modulus (B) of α-Fe, 197.24 GPa is consistent with the theoretical value found by Hung et al[30], 195 GPa, but it is about 17 % larger than the experimental value of 168 GPa[29]. From Table 2 it is clear that B of α-Fe(TM) (TM = Sc, Ti, and V) is smaller than that of α-Fe. The present calculations properly estimate the lattice parameters of dilute alloys of TM (TM = Sc, Ti, and V) in iron, but slightly overestimate the bulk modulus.

3.2 Electronic properties

The total density of states (tDOS) for α-Fe(TM) (TM = Sc, Ti and V) alloys are depicted in Figure 2. The Fermi level is located at 8.2655 eV, 8.3267 eV, and 8.3444 eV, for α-Fe(Sc), α-Fe(Ti), and α-Fe(V), respectively. The calculated Fermi level for α-Fe is 8.3213 eV. In the Figure 2, the Fermi level is taken as zero energy, and the tDOS for α-Fe is included for comparison. The profiles of the tDOS are similar to each other and with that of α-Fe. The large density of states at the Fermi energy is indicative of a spontaneous ferromagnetism. The partial densities of states (pDOS) for Sc, Ti and V impurities in α-Fe are shown in Figure 3. The spin-down density of states is the majority-spin electrons for all impurities. This fact implies that the TM impurities couple antiferromagnetically to the neighboring Fe atoms. The pDOS were also calculated at all nonequivalents iron sites for α- Fe(TM) (TM = Sc, Ti and V). The profile of these pDOS have the same shape, and only the pDOS for Fe1 atoms (the Fe nearest neighbor to TM) in α- Fe(TM) (TM = Sc, Ti and V) alloys are shown to illustrate in Figure 3. As can be seen, the profiles of the pDOS for Fe1 atoms are very similar to that of α-Fe. This result indicates that the presence of the TM impurity at the first coordination shell of Fe1 atoms does not alter significantly the features of their distribution of states.

The electron density (ED) is useful for analyzing the distribution of the electron charge around the different atomic sites of the lattice. In Figure 4 are shown the corresponding

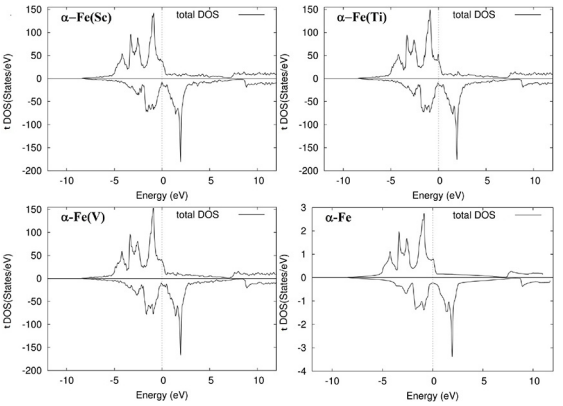

Figure 2. Calculated total density of states (tDOS) for α-Fe(TM) (TM = Sc, Ti and V). The vertical line at zero energy represents the Fermi energy.

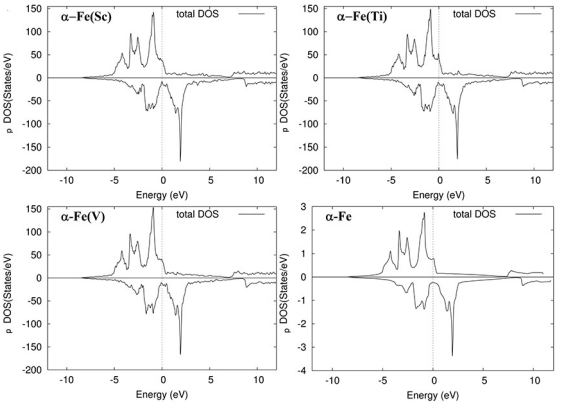

Figure 3. Calculated partial density of states (pDOS) of the TM (Sc, Ti, and V) impurities in α-Fe. The vertical line at zero energy represents the Fermi energy.

ED maps of α-Fe(TM) (TM = Sc, Ti and V) on the (110) crystallographic plane of the bcc cell. The (110) plane contains five of the nonequivalent Fe sites of the crystal structure. The ED map for pure α-Fe is also included (Figure 4(d)) for comparison.

The Figure 4 shows that the ED at the core region of the iron atoms is perfectly symmetric and spherical. The isocurves (curves of constant charge density) indicate that the symmetry of the valence charge distribution of the iron atoms occupying the neighboring sites (Fe1, Fe2 and F3) to impurity is perturbed in relation to pure α-Fe. It is observed little modification in the valence charge distribution for the iron atom at Fe4 site. The isocurves also show that the inclusion of the TM impurity in α-Fe induces a pronounced redistribution of charge on the interstitial region of the lattice between the impurity and the iron atoms' nearest neighbors (Fe1, Fe2 and F3). As can be seen by comparing Figures. 4(a), 4(b) and 4(d) a portion of the delocalized electron charge (characteristic of the metallic bond nature) observed between the Fe sites in α-Fe is transferred to the space around the impurity. It is an indicative of a strong attraction of the

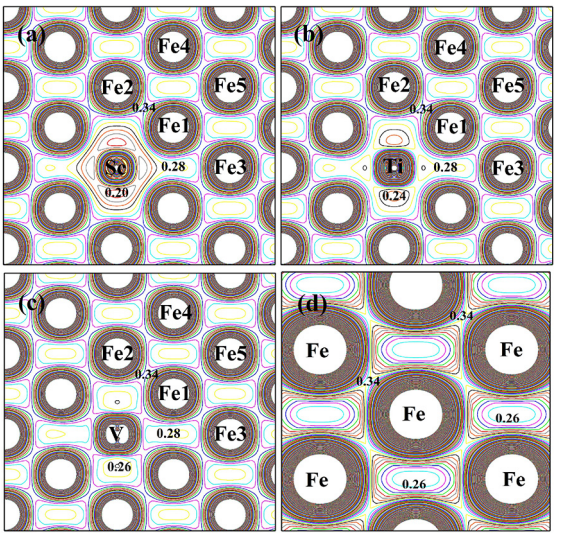

Figure 4. Electron density map in the (110) plane of the bcc structure plotted from 0 e/Å^3 and delta of 0.02 e/Å^3 for: (a) α-Fe(Sc); (b) α-Fe(Ti); (c) α-Fe(V); (d) α-Fe.

conducting electrons by the atomic sphere of the TM impurity. The disturbance caused on the interstitial distribution of charge by the introduction of V in α-Fe (Figure 4(c) is lesser than that due to the introduction of Sc and Ti. These results suggest that the TM impurities are more electropositive than the host iron atoms.

3.3 Magnetic moment

The calculated total magnetic moment per atom (*M*) for α-Fe(TM) (TM = Sc, Ti and V) alloys are 2.130 μ_B/at, 2.129 μ_B/at and 2.138 μ_B/at for TM = Sc, Ti, and V, respectively. The *M* value for α-Fe(Ti) is in good agreement with the experimental measurement of 2.09 μ_B/at for $Fe_{0.972}Ti_{0.028}$ alloy[31]. The value of 2.225 μ_B/at for α-Fe, is slightly larger than the theoretical value found by Rayne et al.[32], 2.20 μ_B/at, and Ali et al.[33], 2.196 μ_B/at, but is in accordance with the experimental value 2.22 μ_B/at.[34].

The calculated magnetic moment (*m*) for TM = Sc, Ti and V, impurities in α-Fe(TM) alloys are -0.289 μ_B, -0.628 μ_B, and -1.129 μ_B, respectively. The *m* values for Ti and V are in good agreement with the experimental values -0.67 μ_B[31] and -0.9 μ_B[35], respectively. The negative sign of these quantities is an indicative that the TM impurities couple antiferromagnetic to the host Fe atoms. This coupling can contribute to reduce the total magnetic moment per atom of α-Fe(TM) (TM = Sc, Ti and V) alloys relative to that of α-Fe. Since, Sc, Ti, and V are not magnetic in pure state it can be concluded that the local magnetic moment observed at the impurity site in bcc-Fe(TM) (TM = Sc, Ti and V) alloys is induced by the host Fe atoms.

Figure 5 shows the calculated local magnetic moment at nonequivalent iron sites in α-Fe(TM) (TM = Sc, Ti and

V) versus *r'* (Table 1). The *r'* dependence of the *m* shows similar behavior for all α-Fe(TM) alloys. For Fe1 the presence of the TM impurity reduces the values of the *m* relative to that of pure α-Fe. This reduction is about 0.11 μ_B for Sc and Ti, and of 0.03 μ_B for V. For the next nearest neighbors Fe2, Fe3 and Fe4, the value of the local magnetic moment varies slightly around 2.225 μ_B. For Fe5 and Fe6 sites (iron sites located at fifth and sixth neighbor shells of TM) *m* shows a slight increase relative to pure α-Fe. The local magnetic moment at Fe7 site is also slightly perturbed, mainly for TM = Sc and Ti.

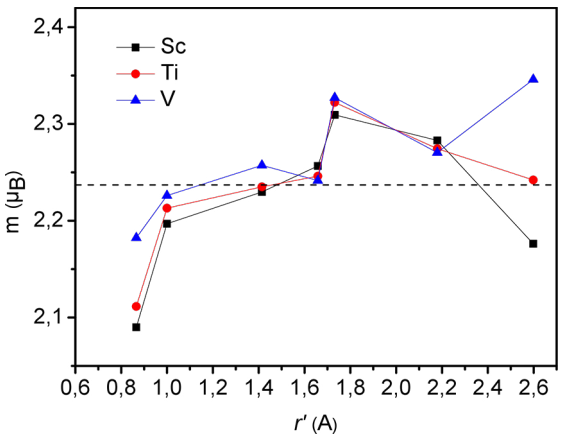

Figure 5. Calculated local magnetic moment (*m*) at non-equivalent irons sites for α-Fe(TM) (TM = Sc, Ti, and V) expressed as function of *r'*. The dashed horizontal line correspond to *m* of pure α-Fe.

3.4 Hyperfine interactions

Figure 6(a) displays the magnetic hyperfine field (H_{hf}) at nonequivalent iron sites in α-Fe(TM) (TM = Sc, Ti and V), as function of *r'*. The dependence of H_{hf} with *r'* is similar for all alloys. The found value of H_{hf} for α-Fe (- 306.0 kG) agrees very well with theoretical data, - 313.2 kG[36], but is lower than the experimental value -339 kG[37].

As can be seen in the Figure 6(a), the presence of the TM impurity leads to a large decrease of H_{hf} in the Fe1 and Fe2 neighbors relative to that of α-Fe. It is noteworthy fact that the hyperfine magnetic field at Fe1 and Fe2 sites in α-Fe(TM) increases as the TM impurity is changed from V, to Ti, and to Sc, while the *m* at these iron sites increase in the following sequence: α-Fe(Sc), α-Fe(Ti), and α-Fe(V). For Fe3, Fe4, Fe5 and Fe6 neighbors, the presence of the TM impurity seems little affect the value of H_{hf}. The hyperfine magnetic field at Fe7 site also appears to be influenced by the presence of the impurity.

The H_{hf} at Sc, Ti, and V atoms in α-Fe(TM) are: -147.62 kG, -141.20 kG and -132.46 kG, respectively. These values are slightly larger than the experimental values -133 kG for Sc[38], -122 kG for Ti[39], and -88 kG for V[37].

The H_{hf} acting on an iron nucleus, in the absence of an external field, can be expressed as a sum of three contributions:

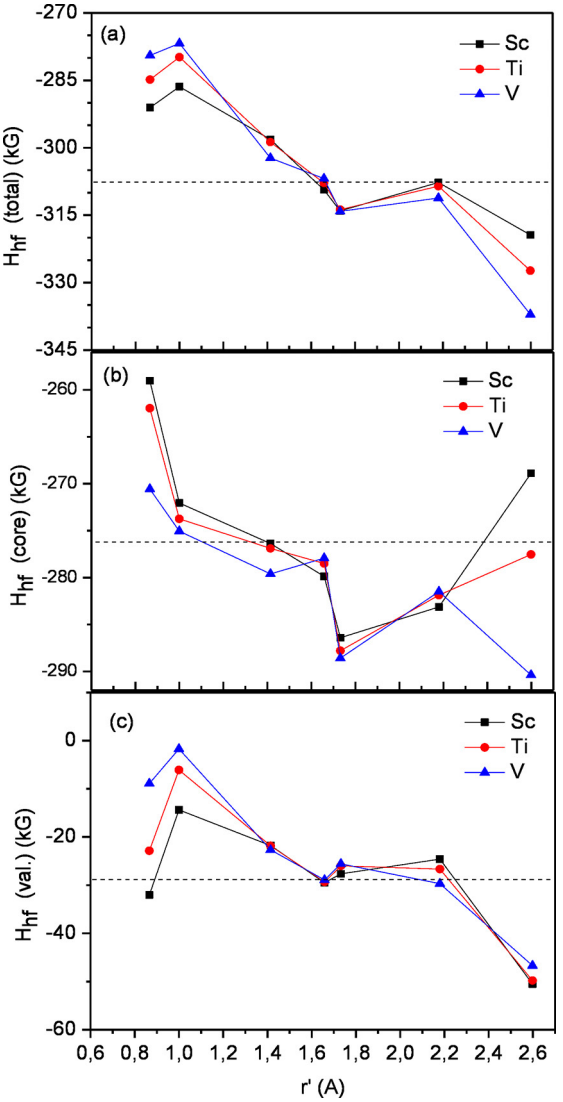

Figure 6. (a) The magnetic hyperfine field (H_{hf}), (b) the core contribution ($H_{hf}(core)$) and (c) the valence contribution ($H_f(val)$) to H_{hf} as function of *r'*. The dashed horizontal lines correspond to the respective values for α-Fe.

the orbital magnetic moment (H_o), the dipole term (H_d) and the Fermi contact term (H_{Fc}). The first two contributions are often small even in the case of ordered alloys, therefore, a good approximation for H_{hf} is:

$$H_{hf} = H_{Fc} = -\frac{8}{3}\pi\gamma_N[|\Psi_{\uparrow(0)}|^2 - |\Psi_{\downarrow(0)}|^2] \quad (3)$$

In this, γ_N is the nuclear gyromagnetic ratio and $\Psi_{\uparrow(0)}$ and $\Psi_{\downarrow(0)}$ are the densities of the s electrons at the nucleus (r = 0) for up (↑) and down (↓) spins, respectively. The spin density arises partly from core electrons, partly from the conduction 4s electrons and indirectly as a result of the polarization effects on the filled s orbitals by unpaired d electrons. Then, H_{hf} can be regarded as consisting of two contributions: $H_{hf}(core)$ representing the field due to polarization of the core (1s, 2s,

3s) electrons and $H_{hf}(val)$ representing the one due to the polarization of valence (4s, 3d, 4p) electrons.

$H_{hf}(core)$ and $H_{hf}(val)$ contributions to H_{hf} at nonequivalent iron sites in α-Fe(TM) (TM = Sc, Ti and V) as function of *r'* are shown in Figure 6(b) and 6(c). $H_{hf}(core)$ is the dominant contribution to H_{hf} at all Fe sites. A linear correlation between $H_{hf}(core)$ and the local magnetic moments is observed at all Fe sites (Figure 5 and Figure 6(b)). The calculated proportionality coefficient ($H_{hf}(core)/m_{Fe}$) at Fe1, Fe3, Fe4, Fe5 and Fe6 (about, 124 kG/μ_B) is slightly reduced relative to that of α-Fe (-125.50 kG/μ_B). For irons located at Fe2 and Fe7 sites $H_{hf}(core)/m_{Fe}$ varies slightly about 123.7 kG/μ_B. These results are consistent with previous theoretical calculations that indicated that $H_{hf}(core)$ for Fe is proportional to the 3d shell magnetic moment[40,41]. $H_{hf}(core)$ at TM = Sc, Ti and V are 23.63 kG, 71.95 kG and 166.06 kG, respectively. The $H_{hf}(core)$ value for Sc is in very good agreement with the experimental value of 20 kG[38]. Similar to the Fe atoms in α-Fe, the $H_{hf}(core)$ of the TM in α-Fe(TM) alloys is antiparallel to the magnetic moment, i.e., a negative magnetic moment corresponding to a positive $H_{hf}(core)$.

The $H_f(val)$ contributions to the Fermi contact field, consists of two parts: the self-polarization valence hyperfine field due to the s–d exchange interaction within the atom and the transferred valence hyperfine field which arises due to s–d hybridization between the s orbitals of the atom and the spin polarized d orbitals of the neighboring atoms. Despite the $H_{hf}(val)$ contribution to H_{hf} be small, the magnitude of $H_{hf}(val)$ depends sensitively of the local atomic environment and provides important information about the electronic structure of neighboring atoms[42]. The profile of the curve $H_{hf}(val)$ *vs r'* (Figure 6(c)) is similar to that of H_{hf} *vs r'* (Figure 6(a)). At all Fe sites the $H_f(val)$ value is negative which in turn leads to an increase of the absolute H_{hf} value relatively to $H_{hf}(core)$. In α-Fe(Sc), for example, although the first near neighbors (Fe1 and Fe2) show the lower $H_{hf}(core)$ values in the α-Fe(TM) (TM = Sc, Ti and V) alloys, the higher $H_f(val)$ values at these sites lead to larger absolute H_{hf} values. For Fe3, Fe4, Fe5 and Fe6 sites the values of $H_f(val)$ are close to the corresponding value of α-Fe for all α-Fe(TM) (TM = Sc, Ti and V) alloys.

$H_{hf}(val)$ at TM = Sc, Ti and V are -171.25 kG, -213.15 kG and -298.47 kG, respectively. The $H_{hf}(val)$ value for Sc is close to the experimental value -150 kG[38]. As can be observed $H_{hf}(val)$ is the dominant contribution to H_{hf} for all TM in α-Fe(TM). As the TMs selected here have no magnetic moment in pure state this result indicates that there is a strong interaction between the distributed charge in the interstitial region of the lattice and the valence electrons of the TM atoms.

In order to better understand the charge distribution in α-Fe(TM) (TM = Sc, Ti and V) alloys additional calculations were performed to determine the isomer shift (*IS*). The origin of *IS* lies in the finite size of the nucleus. The electric monopole interaction between the nuclear charge and the electrons at the nucleus shifts nuclear energy levels without changing the degeneracy. This interaction arises due to the size effect of the nucleus during the excitation of the nucleus, the charge distribution and the effective radius change and therefore the shift of the energy levels of the ground state and excited state are different. This shift cannot be measured directly, thus a suitable reference such as a specific source or an absorber is necessary. To investigate the electron density at the Fe nucleus the *IS*, relative to the bcc-Fe, was calculated.

The Mössbauer spectroscopy is a powerful tool to study the *IS*. The *IS* is influenced by the oxidation state of the atom through the occupation number of the electronic orbital and can be calculated using the following expression:

$$IS = \alpha[\rho_n(0) - \rho_s(0)] \quad (4)$$

where $\rho_n(0)$ is the electron density on the sample nucleus and $\rho_s(0)$ is the electronic density on the source nucleus. In this expression

$$\alpha = \beta\Lambda r^2 \quad (5)$$

where β is characteristic of the Mössbauer isotope. Although the magnitude β must be evaluated from nuclear calculations, the constant α can be estimated by calibration[43-45] and the *IS*, in mm/s, can be estimated through the results obtained from the first principles calculations.

The Figure 7 displays the isomer shift (*IS*) at all nonequivalent iron sites in α-Fe(TM) (TM = Sc, Ti and V) plotted versus *r'*. The calculated *IS* values at Fe1 and Fe2 sites are negative showing that these iron atoms experience a higher nuclear electron density than that in the α-Fe. For Fe atoms, the principal influence on the Fe isomer shift occurs through the outermost occupied s-orbital then a negative *IS* implies an increase in s-electron density at the nucleus. For iron sites located farther away from the impurity (Fe3-Fe7) the values of the *IS* increase positively indicating that the s-electron density at the iron nucleus decreases relative to α-Fe. The principal influence on the Fe isomer shift occurs through the outermost occupied s-orbital, but the 3d-electrons can also influence the nuclear electron density. The shielding of the s-orbital by other electrons (3d) increases the s-radial functions and decreases the s-density at the nucleus, causing a more positive *IS*. Hence, the difference observed in the isomer shift values among the nonequivalent iron sites can also indicate disturbance in the number of s-electron charge or in the shape of the spatial distribution of the 3d orbitals of the iron atoms (relatively to that in bcc-Fe).

To investigate the local site symmetry effect on the electronic structure of the iron atoms in α-Fe(TM) (TM = Sc, Ti and V), the electric field gradient (EFG) was calculated. The EFG is the negative second derivate of the potential at the probe nucleus of all surrounding electric charge. The

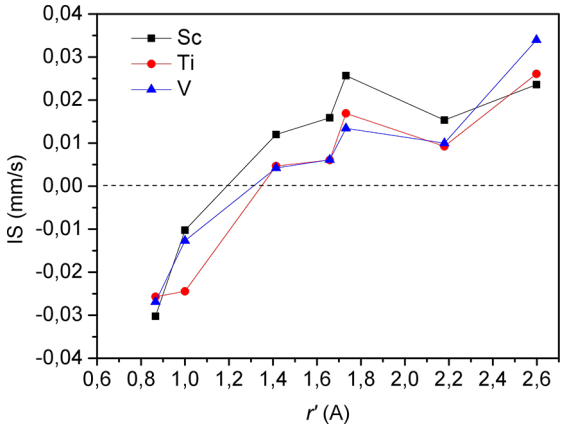

Figure 7. Isomer shift (IS) values at nonequivalent iron sites plotted as function of *r'*. The dashed horizontal lines correspond to the IS value of α-Fe.

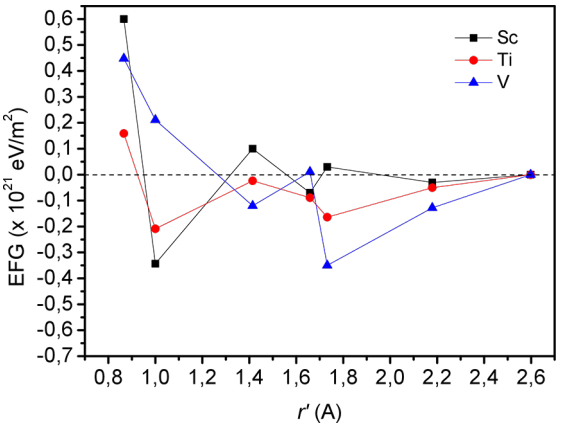

Figure 8. Electric field gradient at nonequivalent iron sites plotted as function of *r'*.

Laplace equation requires the EFG to be traceless tensor. Consequently, only two independent parameters are needed to specify the EFG completely, and the two which are usually chosen are the component with the largest magnitude of the EFG (V_{zz}) and the asymmetry parameter η ($0 \leq \eta \leq 1$) defined by the magnitude of V_{xx} - V_{yy} / V_{zz} with $|V_{zz}| \geq |V_{yy}| \geq |V_{xx}|$. In two special cases, when the probe nucleus is placed in an environment with cubic or axial symmetry, the number of parameters describing the EFG tensor can be reduced. In the first case, the EFG completely vanishes, and in the second one, η = 0, i.e. $V_{xx} = V_{yy}$.[46]

The EFG is an important ground state property of a solid and depends sensitively on the asymmetry of the electronic charge density near the probe nucleus in a crystal. It therefore embraces contributions from both the valence electrons of the atom and from surrounding atoms. Generally, the valence contribution is the main contribution to the EFG.

The EFG values for all nonequivalent iron sites in the crystal lattice of α-Fe(TM) (TM = Sc, Ti and V) are displayed in Figure 8. The iron atoms located at the vertices of the supercell (Fe7) and the TM atom occupying the central position of the lattice have local cubic symmetry and consequently, zero EFG. The EFG value is larger for iron atoms nearest neighbors (Fe1 and Fe2) to TM, and decreases (but, EFG ≠0) for iron atoms at more distant sites (Figure 8). The *r'* dependence of the EFG shows an irregular behavior for all α-Fe(TM) (TM = Sc, Ti and V) alloys. The EFG has axial symmetry (η = 0) in the Fe1, Fe2, Fe5, and Fe6 sites in all the studied alloys. The asymmetry parameter values for Fe3 sites are 0.3, 0.49, and 0.38, and for Fe4 sites are 0.1, 0.41, and 0.74 for α-Fe(Sc), α-Fe(Ti) and α-Fe(V), respectively. As, for iron atoms the main contribution to the EFG comes from the valence electrons, the observed variation of the EFG values can be an indicative that at nonequivalent iron sites the electronic population of the 3d and 4s orbitals is different.

Figure 9 shows the calculated total charge confined inside the atomic sphere at all nonequivalent iron sites for α-Fe(TM) (TM = Sc, Ti and V) alloys. As can be observed, the total charge of the iron atoms is increased upon introduction of the TM impurity in α-Fe. The increase of charge is relatively larger for iron atoms located at the nearest neighbors to TM impurity. The increase is of about 0.06 for the irons at the Fe1 sites, and is of about 0.04 for irons at Fe2 sites. For iron atoms at the next shells of neighbor (from 3th till 7th), the increase of the total charge is less and depends on the impurity. The total charge at these sites also shows slight fluctuation of values, and the increase is of about 0.03, in α-Fe(V), 0.02 in α-Fe(Ti), and 0.01 in α-Fe(Sc). The charge inside the atomic sphere of Sc, Ti, and V is reduced in 1.656, 1.716, and 1.655, respectively, when going from the neutral atom to the supercell structure of α-Fe(TM) (TM = Sc, Ti and V) alloys. The increase of the total charge inside the atomic sphere of the iron atoms in α-Fe(TM) (TM = Sc, Ti and V) changes the number of 3d and 4s electrons (relative to bcc-Fe). The change in 3d electron density leads to variations on the magnetic moment of the iron atoms, and the fluctuations of the 4s electron density can to lead to changes on the isomer shift. The isomer shift measures the total s-electron density at the iron nucleus. However, the isomer shift value in compounds depends mainly upon the 3d configuration of iron involved, i.e. an increased 4s electron density increases the s density at the iron nucleus while an increased 3d electron density decreases due to enhanced shielding of the 3d electrons. On the other hand, the change in the magnetic moment of the iron atom affects directly the magnetic hyperfine field at the iron nucleus, as well as the change in the symmetry of charge density around the nucleus modifies the EFG. Hence, for iron atoms located at Fe1 and Fe2 sites, the relative decrease (with respect to α-Fe) of the H_{hf}, $H_{hf}(core)$, and *m*, and the negative *IS* values can be attributed to an increase in the 4s electron density inside the atomic sphere. For iron atoms located from Fe3 to Fe7 sites the relative increase of the H_{hf}, $H_{hf}(core)$, and *m*, and the positive *IS* values can be attributed to an increase in the 3d electron density.

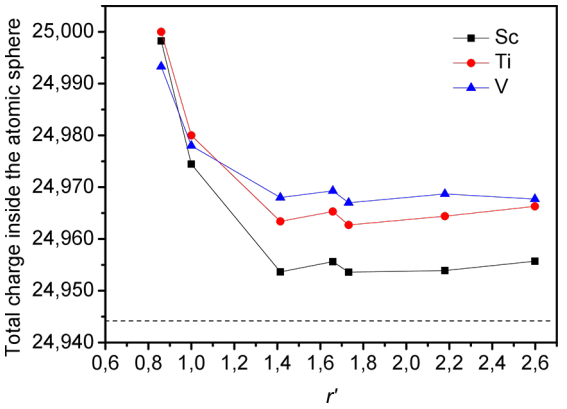

Figure 9. Total charge inside the atomic sphere of all iron atoms plotted as function of *r'*. The dashed horizontal lines correspond to the total charge of iron in α-Fe.

4. Conclusion

The LAPW method, as implemented in the Wien2k computational code, was used to investigate the effect of impurities of 3d TM (Sc, Ti, and V) in the ground state properties of Fe atoms in α-Fe. Special attention was devoted to the electronic effect of the impurity on the change of the hyperfine interactions at the nuclei of the host iron atoms.

From the equilibrium cohesive energy point of view, all the α-Fe(TM) (TM = Sc, Ti and V) alloys are ferromagnetic, and the stability is slightly higher than that of pure α-Fe. The lattice constant of α-Fe slightly increases upon introduction of the TM impurities. The calculated density of states and local magnetic moment for TM = Sc, Ti and V (-0.289 μ_B, -0.628 μ_B, and -1.129 μ_B, respectively) show that the TM impurities couple antiferromagnetic to the host Fe atoms. Since the TM = Sc, Ti, and V, are not magnetic in pure state concluding that the local magnetic moment is induced by the host Fe atoms. The antiferromagnetic coupling between the local magnetic moments of the TM and the iron atoms reduce the total magnetic moment per atom of the supercell (2.130 μ_B/at, 2.129 μ_B/at, and 2.138 μ_B/at for α-Fe(Sc), α-Fe(Ti), and α-Fe(V), respectively) relative to that of α-Fe (2.22 μ_B/at). The magnetic moments of iron atoms located at all nonequivalent sites also vary. For iron atoms nearest neighbors to TM the magnetic moment, decreases while for iron atoms located from Fe3 to Fe7 sites the moment increases. The electron density maps show that the introduction of the TM impurities in α-Fe induces a change on the symmetry of the valence charge distribution of the iron atoms occupying the nearest neighbors sites (Fe1, Fe2 and F3) to impurity. The isocurves also show a prominent redistribution of charge on the interstitial region between the TM impurity and the iron atoms nearest neighbors (Fe1, Fe2 and F3). Furthermore, the calculated total charge indicates an increase on the number of charge in the atomic sphere of the irons atoms. The increase of the total charge inside the atomic sphere of iron atoms affects directly the hyperfine interactions at the iron nuclei. The magnetic field in the iron atoms' nearest neighbors to TM increases, while for irons farthest from the location of the impurity, increases. The isomer shift at iron atoms near the impurity is more negative than that in α-Fe while for iron far from the impurity it is more positive. On the other hand, the EFG's value varies irregularly from one iron site to another, being larger for iron atoms nearest neighbors (Fe1 and Fe2), and decreasing for more distant iron atoms.

The results of this study suggest that the introduction of a TM (TM = Sc, Ti, and V) impurity into α-Fe increases the size of the crystal lattice as well as altering electronic charge distribution of host iron atoms. The increase of the lattice disturbs the position of the iron atoms and the change in the electron density disturbs the hyperfine interactions at all iron nuclei. Disturbances are larger for iron atoms near to impurity and diminish (but not disappear) for farthest irons. At the atomic level the magnetic behavior of the iron atoms in α-Fe(TM) (TM = Sc, Ti and V) alloys cannot be interpreted as a simple dilution process.

5. References

1. Klueh RL, Nelson AT. Ferritic/martensitic steels for next-generation reactors. *Journal of Nuclear Materials*. 2007;371(1-3):37-52.

2. Hasegawa H, Pettifor DG. Microscopic theory of the Temperature-Pressure Phase Diagram of Iron. *Physical Review Letters*. 1983;50:130-133.

3. Mohn P. Theoretical aspects of hyperfine interactions. *Hyperfine Interactions*. 2000;128(1):67-78.

4. Bulanov VY, Dorogina GA. Effect of impurities in iron powders on the physical properties of sintered magnetically soft materials. *Powder Metallurgy and Metal Ceramics*. 1998;37(11):597-601.

5. Dubiel SM, Zinn W. Application of Mössbauer effect in the investigation of the substitution induced spin and charge density changes in bcc-iron. *Journal of Magnetism and Magnetic Materials*. 1984;45(2-3):298-304.

6. Yoshida Y, Nasu S, Fujita FE, Maeda Y, Yoshida H. ^{57}Fe Mössbauer study on point defect in pure α-Fe. *Journal of Magnetism and Magnetic Materials*. 1983;31-34(Pt 2):753-754.

7. Dubiel SM, Zinn W. Influence of V on the Fe site spin and charge densities in BCC-Iron. *Journal of Magnetism and Magnetic Materials*. 1983;37(3):237-247.

8. Williams AR, Moruzzi VL, Gelatt Jr CD, Kübler J. Theory of Invar and Heusler alloys. *Journal of Magnetism and Magnetic Materials*. 1983;31-34(Pt 1):88-94.

9. Paduani C. Electronic structure and magnetic properties of bcc-Fe-Ni alloys. *Physica Status Solid B*. 2003;240(3):634-639.

10. Ustinovshikov Y, Shabanova I. A study of microstructures responsible for the emergence of the invar and permalloy effects in Fe–Ni alloys. *Journal of Alloys and Compounds*. 2013;578:292-296.

11. Rahman G, Kim IG. A First-principles Study on Magnetic and Electronic Properties of Ni Impurity in bcc Fe. *Journal of Magnetics*. 2008;13(4):124-127.

12. Freeman AJ, Wimmer E. Density Functional Theory as a Major Tool in Computational Materials Science. *Annual Review of Materials Science*. 1995;25:7-36.

13. Anisimov VI, Antropov VP, Liechtenstein AI, Gubanov VA, Postnikov AV. Electronic structure and magnetic properties of *3d* impurities in ferromagnetic metals. *Physical Review B*. 1988;37(10):5598-5602.

14. Akai H, Akai M, Kanamori J. Electronic Structure of Impurities in Ferromagnetic Iron. II. 3d and 4d Impurities. *Journal of the Physical Society of Japan*. 1985;54(11):4257-4264.

15. López-Cháves E, Martinez Magadán JM, Castillo-Alvarado FL. Effect of Ni and Co impurities on the electronic structure and magnetic properties of BCC iron. *Journal of Magnetism and Magnetic Materials*. 2004;280(2-3):293-303.

16. Park JH, Youn SJ, Min BI, Cho HS. Electronic structure and magnetic properties of 3d and 4d transition-metal impurities in ferromagnetic Fe. *Journal of the Korean Physical Society*. 2000;36(1):34-41.

17. You Y, Yan MF. Interactions of foreign interstitial and substitutional atoms in bcc iron from *ab initio* calculations. *Physica B: Condensed Matter*. 2013;417:57-69.

18. Medvedeva NI, Murthy AS, Richards VL, van Aken DC, Medvedeva JE. First principle study of cobalt impurity in bcc Fe and Cu precipitates. *Journal of Materials Science*. 2013;48(3):1377-1386.

19. Nonas B, Wildberger K, Zeller R, Dederichs PH. Ab-Initio calculations for 3d impurities on Fe(001) and Ni(001). *Journal of Magnetism and Magnetic Materials*. 1997;165(1-3):137-140.

20. Liu XJ, Yu P, Wang CP, Ishida K. Thermodynamic evaluation of Co-Sc and Fe-Sc systems. *Journal of Alloys and Compounds*. 2008;466(1-2):169-175.

21. Paduani C, Krause JC. Electronic structure and magnetization of Fe-Co alloys and multilayers. *Journal of Applied Physics*. 1999;86:578-583.

22. Błachowski A, Wdowik UD, Ruebenbauer K. Volume effect and electron band modification in α-Fe by substitutional impurities. *Journal of Alloys and Compounds*. 2009;485(1-2):36-40.

23. Błachowski A. Charge and Spin Density Perturbation on Iron Nuclei by Non-Magnetic Impurities Substituted on the Iron Sites in *α*-Fe. *Acta Physica Polonica A*. 2008;114(6):1563-1571.

24. Jones RO. Density functional theory: its origins, rise to prominence, and future. *Reviews of Modern Physics*. 2015;87(3):897-923.

25. Perdew JP, Burke K, Ernzerhof M. Generalized Gradient Approximation Made Simple. *Physical Review Letters*. 1996;77(18):3865-3868.

26. White JA, Bird DM. Implementation of gradient-corrected exchange-correlation potentials in Car-Parrinello total-energy calculations. *Physical Review B, Condensed Matter*. 1994;50(7):4954-4957.

27. Blaha P, Schwarz K, Luitz J. *Computer code WIEN97*. Wien: Technische Universität Wien; 1997.

28. Weissmann M, García G, Kiwi M, Ramírez R, Fu CC. Theoretical study of iron-filled carbon nanotubes. *Physical Review B*. 2006;73:125435.

29. Herper HC, Hoffmann E, Entel P. *Ab initio* full-potential study of the structural and magnetic phase stability of iron. *Physical Review B*. 1999;60(6):3839-3848.

30. Hung A, Yarovsky I, Muscat J, Russo S, Snook I, Watts RO. First-principles study of metallic iron interfaces. *Surface Science*. 2002;501(3):261-269.

31. Kajzar F, Parette G. Magnetic moment distribution in bcc Fe-Ti Alloys. *Solid State Communications*. 1979;29(4):323-327.

32. Rayne JA, Chandrasekhar BS. Elastic Constants of Iron from 4.2 to 300°K. *Physical Review*. 1961;122(6):1714-1716.

33 Ali K, Arya A, Ghosh PS, Dey GK. A first principles study of the cohesive, elastic and electronic properties of binary Fe-Zr intermetallics. *Computational Materials Science*. 2016;112(Pt A):52-66.

34. Collins MF, Low GG. Neutron diffraction studies of magnetic moments in dilute transition metal alloys. *Journal de Physique*. 1964;25(5):596-600.

35. Campbell IA. The magnetic moment distributions for transition metal impurities in iron. *Proceedings of the Physical Society*. 1966;89(1):71.

36. Michalecki T, Deniszczyk J, Frąckowiak JE. Ab initio study of the effect of pressure on the hyperfine parameters of ^{57}Fe in bcc phase. *Nukleonika*. 2003;48(Suppl 1):S45-S48.

37. Rao GN. Table of hyperfine fields for impurities in Fe, Co, Ni, Gd and Cr. *Hyperfine Interactions*. 1985;26(1-4):1119-1193.

38. Funk T, Brewer WD, Kapoor J, Metz A, Riegel D. Experiments on the Magnetism of Sc Implanted into Metals. *Hyperfine Interactions*. 2001;133(1):253-267.

39. Brandolini F, De Poli M, Rossi-Alvarez C, Savelli C, Vingiani GB. Magnetic hyperfine field of K, Ca, and Ti in iron. *Hyperfine Interactions*. 1978;5(1):127-136.

40. Watson RE, Freeman AJ. Origin of effective fields in magnetic materials. *Physical Review*. 1961;123(6):2027-2047.

41. Dubiel SM. Relationship between the magnetic hyperfine field and the magnetic moment. *Journal of Alloys and Compounds*. 2009;488(1):18-22.

42. Watson RE, Freeman AJ. Unrestricted Hartree-Fock method: electron densities and magnetic form factors for spin polarized Ni^{++}. *Physical Review*. 1960;120(4):1125-1134.

43. Timoshevskii AN, Timoshevskii VA, Yanchitsky BZ. The influence of carbon and nitrogen on the electronic structure and hyperfine interactions in face-centred-cubic iron-based alloys. *Journal of Physics: Condensed Matter*. 2001;13:1051-1061.

44. Häglund J, Fernández Guillermet A, Grimvall G, Körling M. Theory of bonding in transition-metal carbides and nitrides. *Physical Review B*. 1993;48(16):11685-11691.

45. Duff KJ. Calibration of the isomer shift for ^{57}Fe. *Physical Review B*. 1974;9(1):66-72.

46. Kaufmann EN, Vianden RJ. The electric field gradient in noncubic metals. *Reviews of Modern Physics*. 1979; 51(1):161-214.